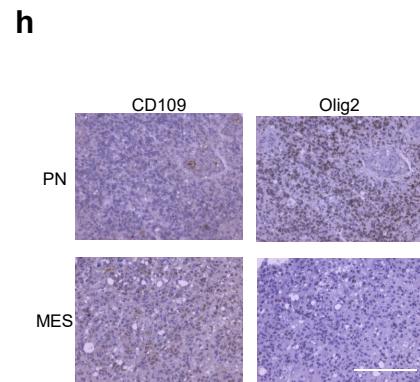
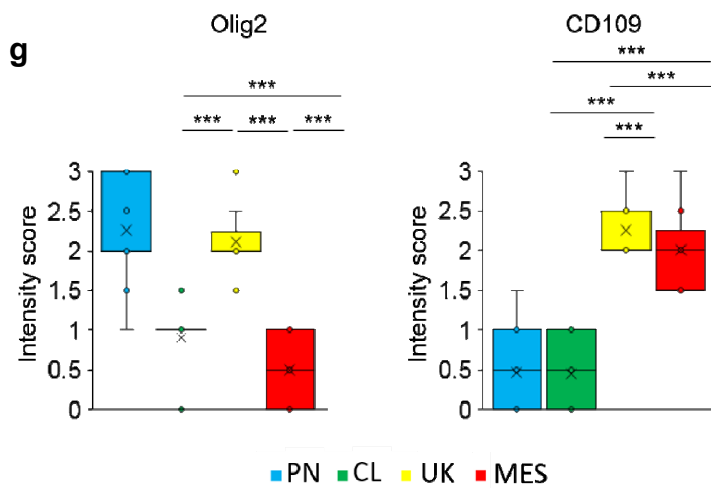
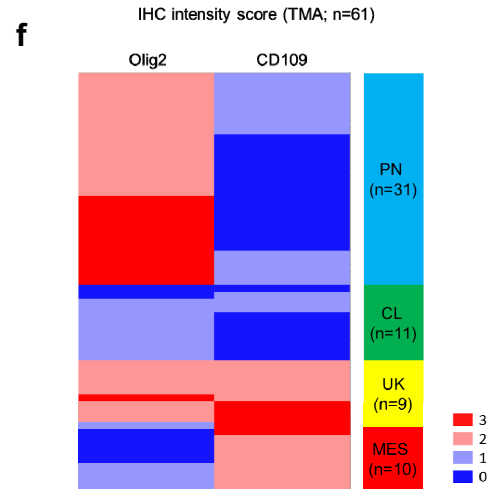
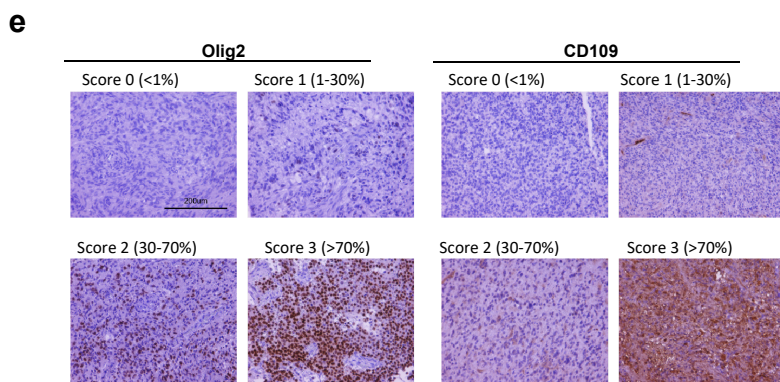
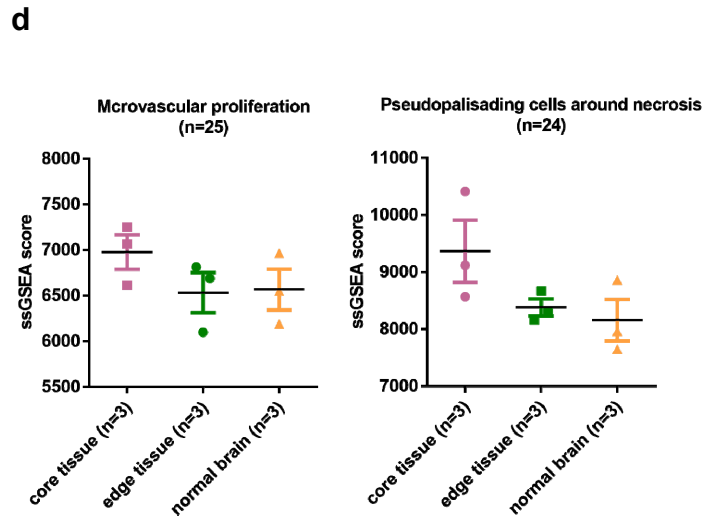
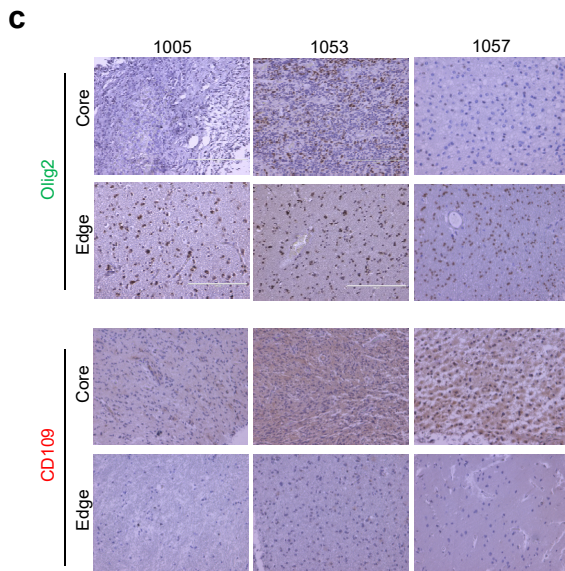
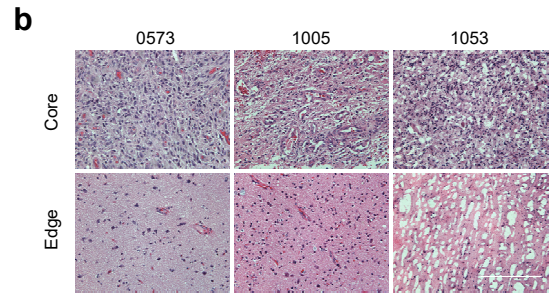
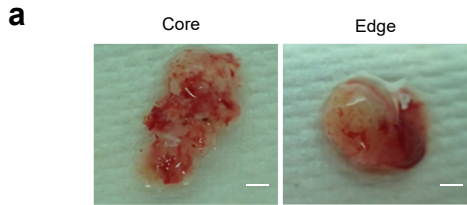


Supplementary information

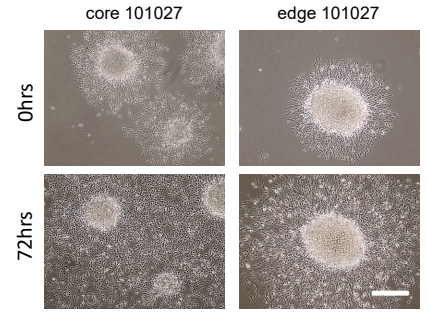
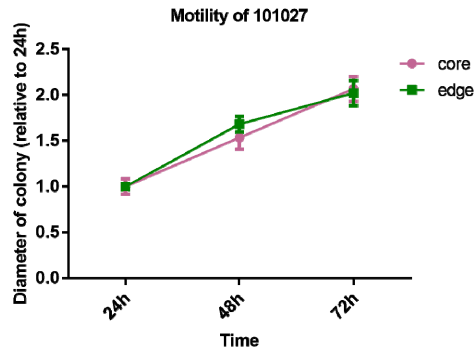
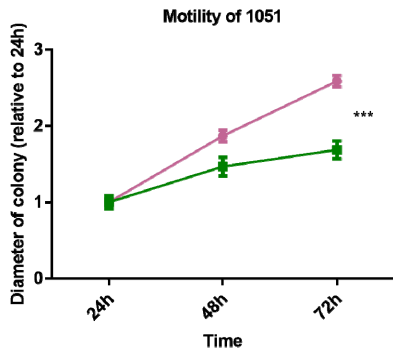
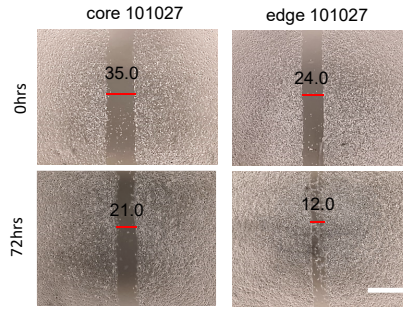
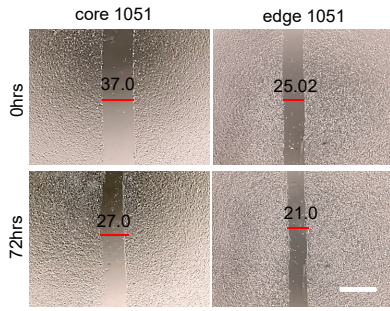
Glioma-initiating cells at tumor edge gain signals from tumor core cells to promote their malignancy

Soniya Bastola, Marat S. Pavlyukov, Daisuke Yamashita, Sadashib Ghosh, Heejin Cho, Noritaka Kagaya, Zhuo Zhang, Mutsuko Minata, Yeri Lee, Hirokazu Sadahiro, Shinobu Yamaguchi, Svetlana Komarova, Eddy Yang, James Markert, Louis B. Nabors, Krishna Bhat, James Lee, Qin Chen, David K. Crossman, Kazuo Shin-Ya, Do-Hyun Nam, and Ichiro Nakano

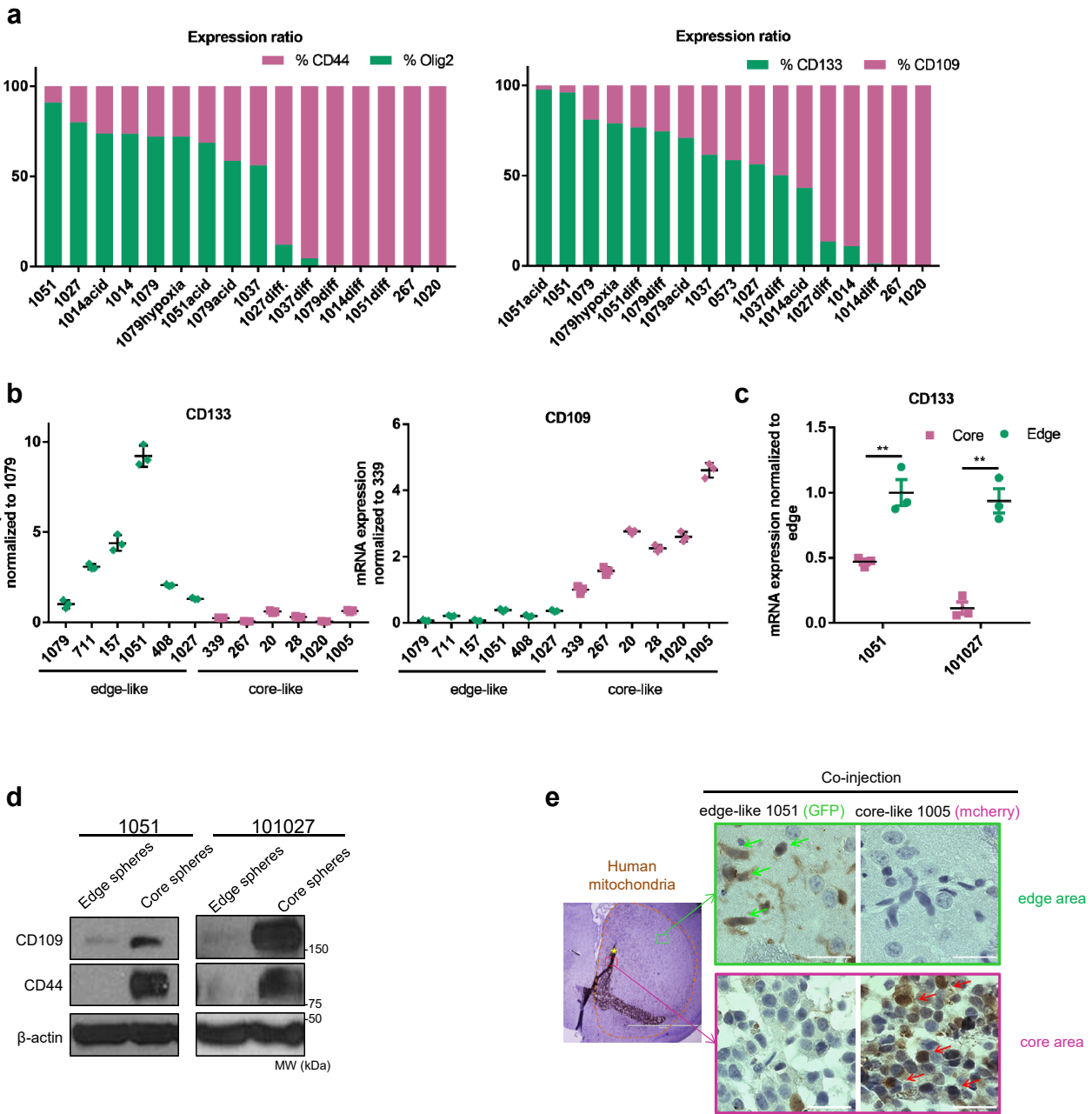
Supplementary Figures 1 - 9



Supplementary Figure 1 GBM cells at the invading edge exhibit distinct molecular signature from those localized in the core. **a** Representative surgical specimens of core and edge tissues from patient #101027. Scale bar 1 mm. **b** H&E staining of edge (lower) and core (upper) tumor tissue from three GBM patients. Scale bar 200 μ m. **c** IHC staining of paired edge and core tumor tissues for Olig2 (upper) and CD109 (lower). Scale bar 200 μ m. **d** Single sample gene set enrichment analysis (ssGSEA) of normal brain, edge and core tumor tissues using microvascular proliferation (MVP) and pseudo-palisading cells around necrosis (PAN) gene signatures from Ivy Glioblastoma Atlas Project database. $n = 3$ independent samples per group. Data are mean \pm s.d. **e** Representative IHC staining of human GBM tissues for Olig2 (left) and CD109 (right) illustrating different staining intensities. Scale bar 200 μ m. **f** Heatmap showing the staining intensity of Olig2 and CD109 in all three subtypes of GBM, $n = 61$. **g** Quantification of IHC staining intensity for Olig2 and CD109 of GBM samples obtained from 61 patients and related to proneural ($n = 31$ independent samples), classical ($n = 11$ independent samples), unknown ($n = 9$ independent samples) and mesenchymal ($n = 10$ independent samples) subtypes. The line in the box is the median, the left and right of the box are the first and third quartiles, and the whiskers extend to 10th and 90th percentiles respectively. *** $p < 0.001$ using one-way ANOVA followed by Tukey's posttest. **h** IHC staining of PN and MES GBM tumor tissues for Olig2 and CD109. Scale bar 200 μ m.

a**b**

Supplementary Figure 2 *In vitro* migration of regionally-specified GBM cells. **a** *In vitro* cell motility assay comparing 1051 and 101027 edge and core sphere colony motility at 24, 48 and 72 hours (left), with representative images (right). Scale bar 100 μm . *** $p < 0.001$ using unpaired, two-tailed t test. Data are mean \pm s.d; $n = 3$ independent samples per group. **b** Wound healing assay comparing core (left) and edge (right) 1051 sphere migration after 72 hours. Scale bar 200 μm .

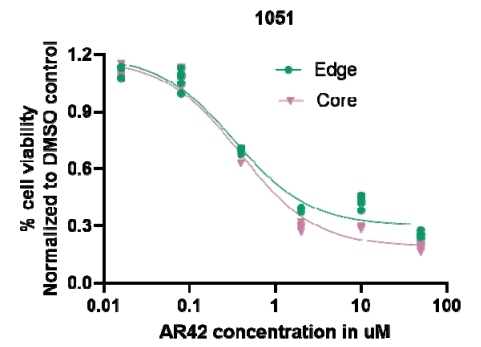
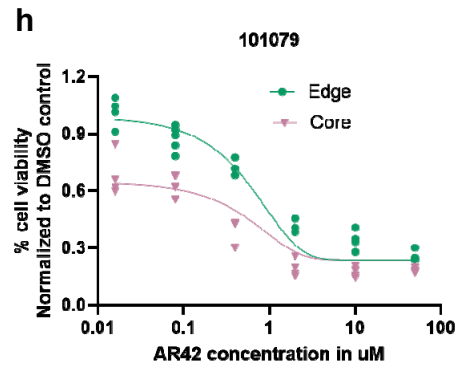
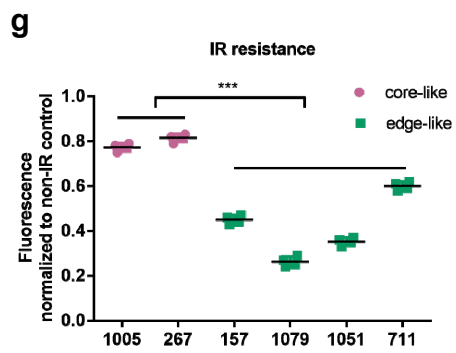
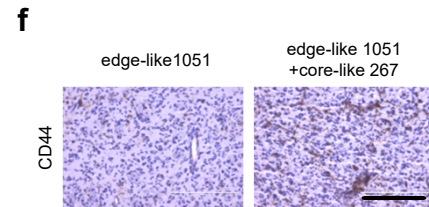
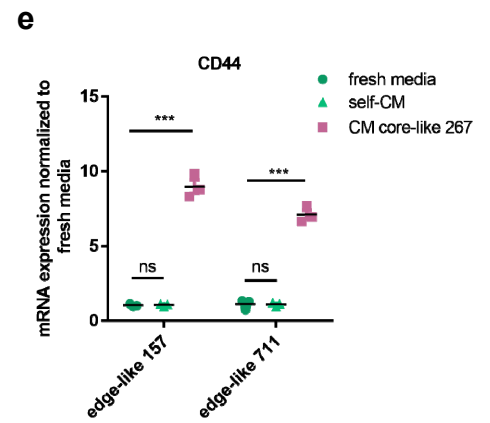
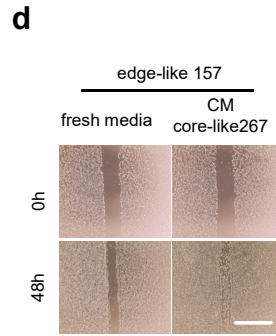
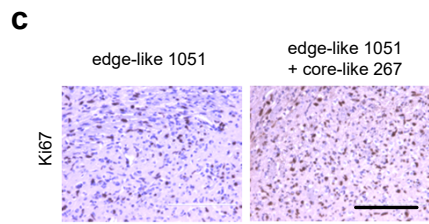
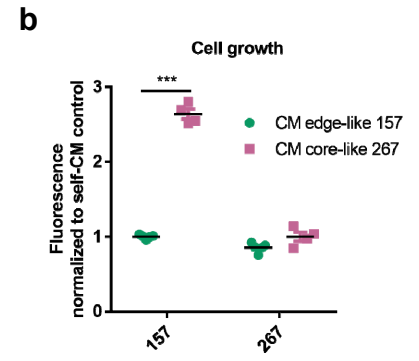
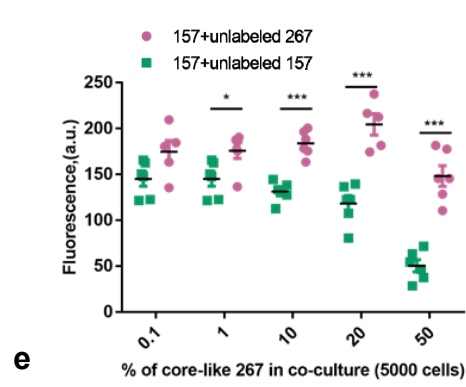
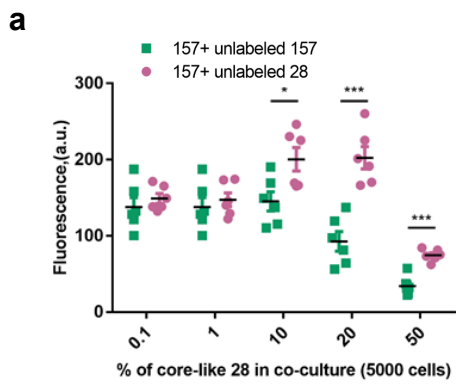


f

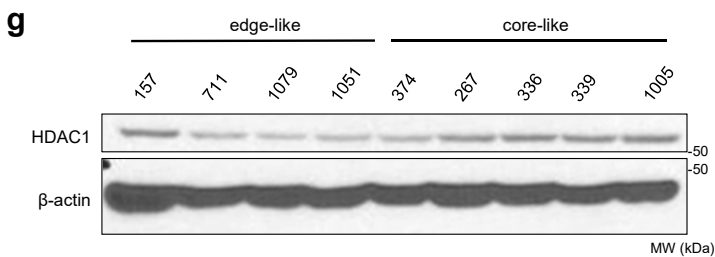
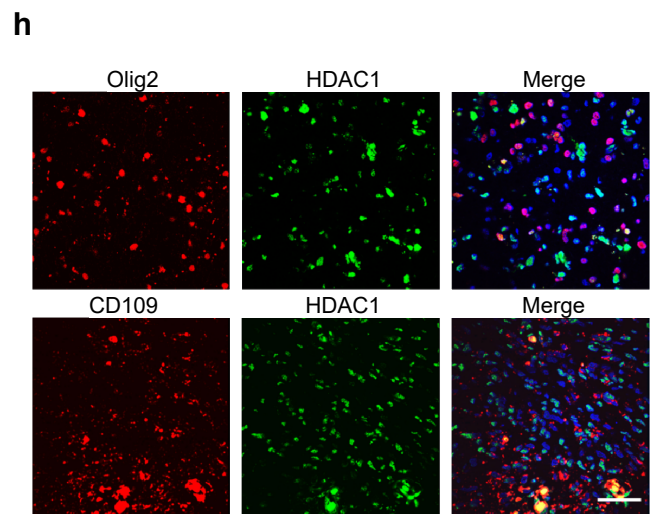
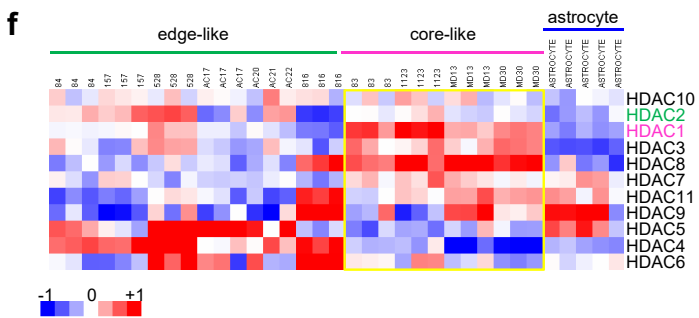
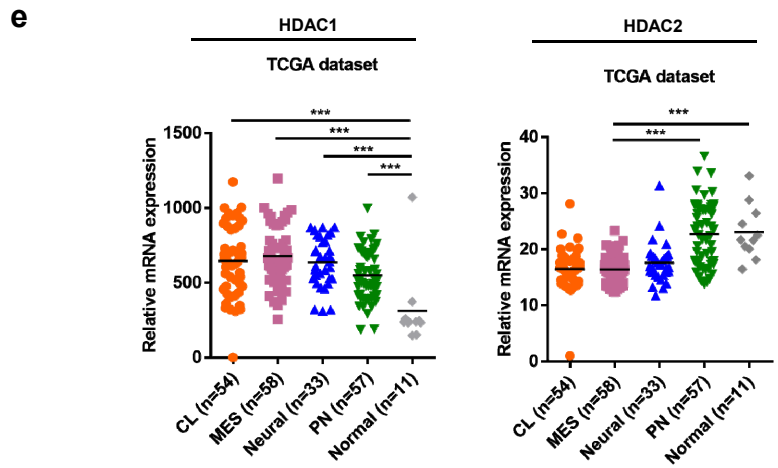
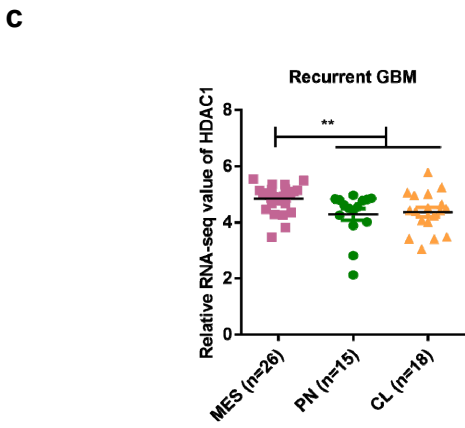
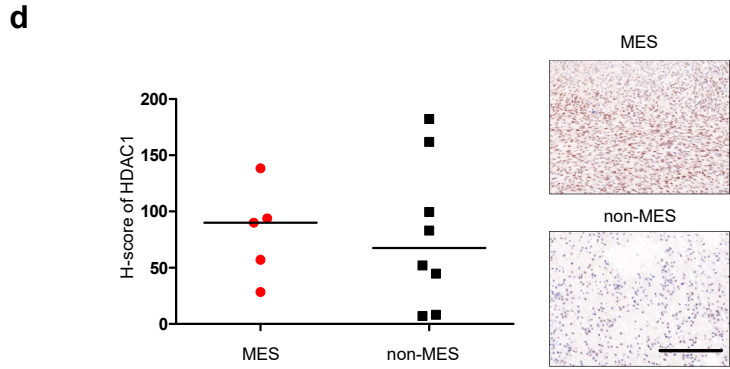
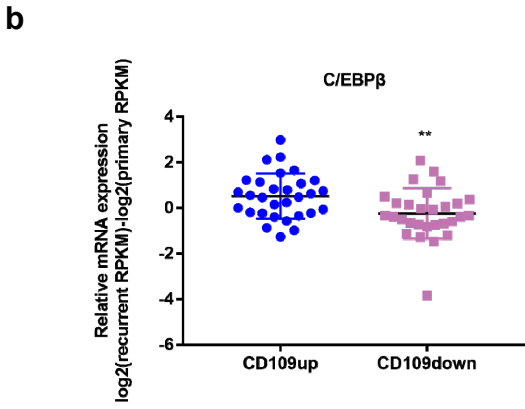
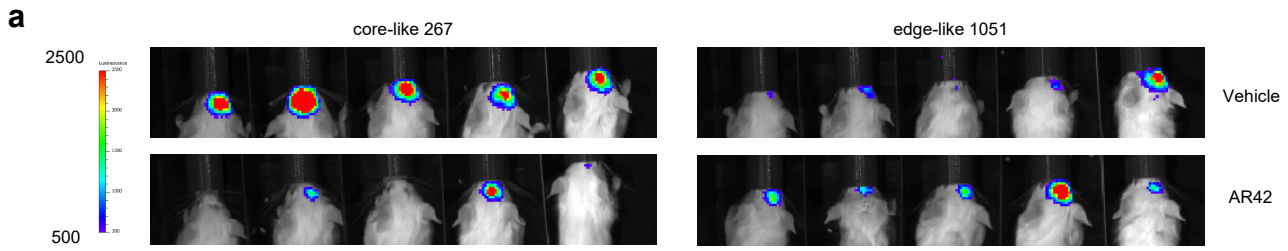
Characteristic of tumor tissues and GBM spheres

	Transcriptional signature		Malignant biological behavior		
	markers	pathways	Infiltration	location preference	IR-resistance
Tissue	edge	Olig2	KRAS	-	-
	core	CD44/CD109	c-MYC/G2M check point	-	-
Spheres	edge-like	CD133	KRAS	high	edge
	edge	CD133	KRAS	high	edge
	core-like	CD109	c-MYC/G2M check point	low	core
	core	CD109	c-MYC/G2M check point	low	core

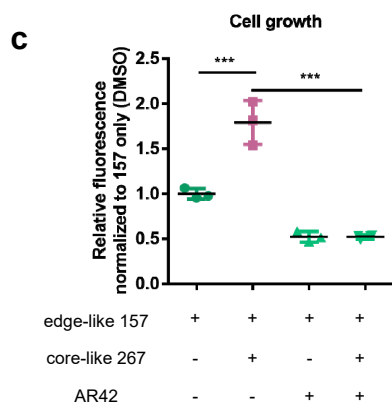
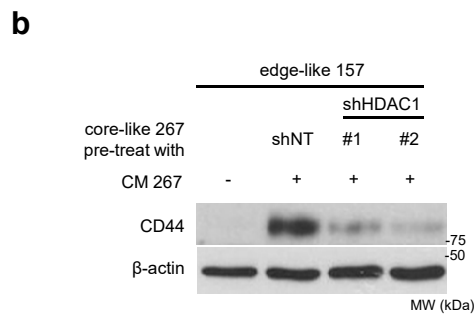
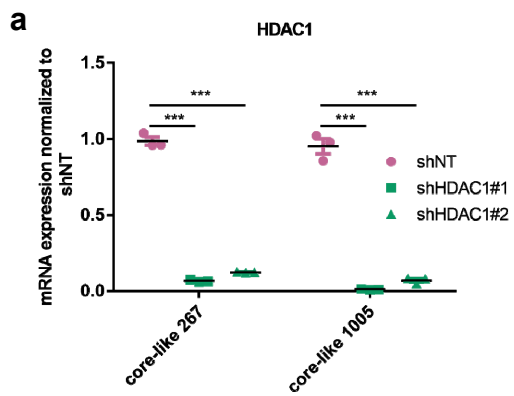
Supplementary Figure 3 Edge-like and core-like GBM sphere lines retain key properties of spatially distinct edge and core GBM. **a** Expression ratio of CD44/Olig2 (left) and CD133/CD109 (right) in various GBM spheres calculated from RNA-seq data. **b** qRT-PCR analysis of CD133 and CD109 expression in six edge-like and six core-like GBM sphere lines. Data are mean \pm s.d.; n = 3 independent samples per group. **c** qRT-PCR analysis of CD133 expression in two edge and two core sphere lines. Data are mean \pm s.d. **p<0.01 using unpaired, two-tailed t test.; n = 3 independent samples per group. **d** WB for CD109 and CD44 using paired 1051 and 101027 edge and core GBM sphere lines. **e** IHC staining for human mitochondria (left), GFP (middle) and mCherry (right) of mouse brain co-injected with edge-like 1051 (GFP labeled) and core-like 1005 (mCherry labeled) GBM spheres at 1:1 ratio. Different regions of the tumor are magnified: edge (upper) and core (lower). Scale bar 2 mm (left) and 20 μ m (right). **f** Table showing the similarity between edge-like/core-like spheres, regionally-defined edge/core spheres and edge/core GBM tumor tissues.



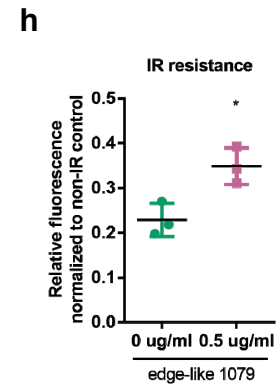
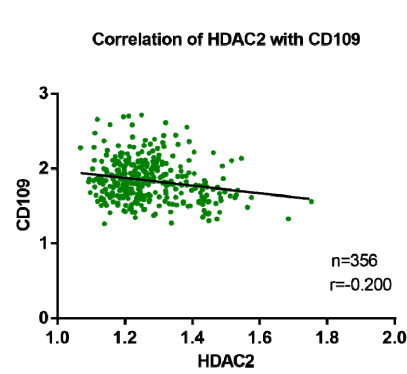
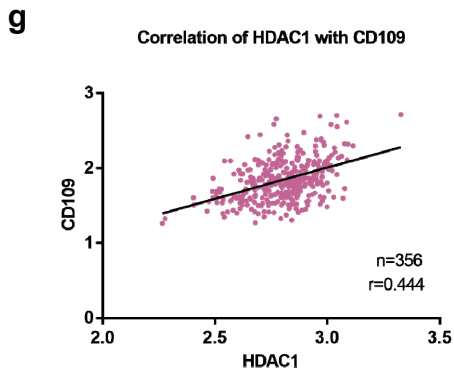
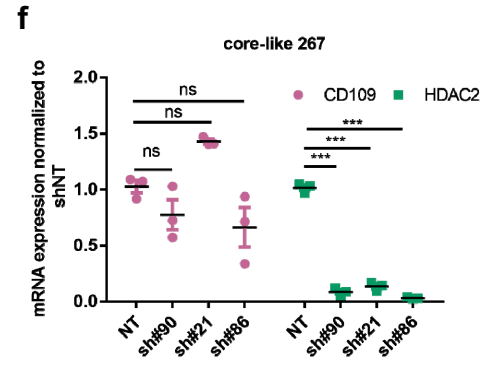
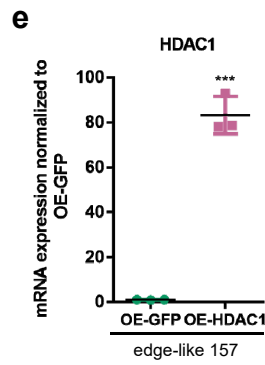
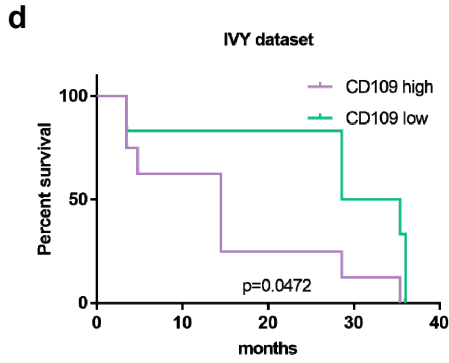
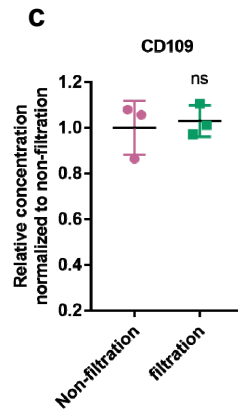
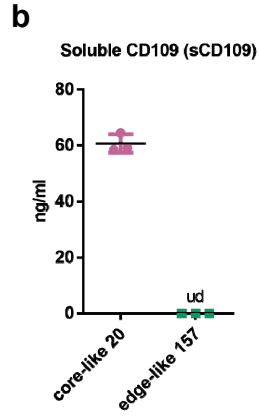
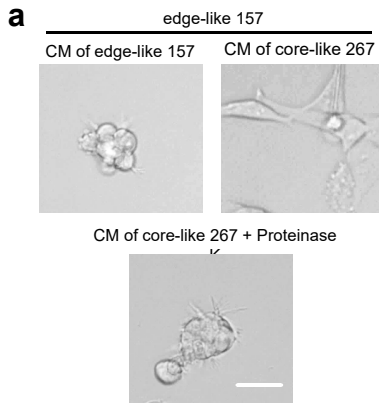
Supplementary Figure 4 Intercellular signaling from core GBM cells provokes aggressiveness of the edge counterparts. **a** Fluorescence intensity of mCherry labeled edge-like 157 GBM spheres co-cultured with increasing amounts of unlabeled edge-like 157 GBM spheres, unlabeled core-like 28 (left) or unlabeled core-like 267 (right) GBM spheres. * $p < 0.05$, *** $p < 0.001$ using unpaired, two-tailed t test. Data are mean \pm s.d.; $n = 6$ independent samples per group. **b** *In vitro* cell growth assay of edge-like 157 and core-like 267 GBM cells treated with CM from edge-like 157 or core-like 267 GBM spheres. *** $p < 0.001$ using unpaired, two-tailed t test. Data are mean \pm s.d.; $n = 5$ independent samples per group. **c** IHC staining for Ki67 of mouse brain intracranially injected with edge-like 1051 GBM spheres alone or with core-like 267 GBM spheres (ratio 95:5). Scale bar 200 μm . **d** Wound healing assay of edge-like 157 GBM spheres treated with/without CM from core-like 267 GBM spheres. Scale bar 100 μm . **e** qRT-PCR analysis of CD44 expression using edge-like 157/711 GBM spheres treated with/without CM from core-like 267 GBM spheres. *** $p < 0.001$ using one-way ANOVA followed by Dunnett's posttest. Data are mean \pm s.d.; $n = 3$ independent samples per group. **f** IHC staining for CD44 of mouse brain intracranially injected with edge-like 1051 GBM spheres alone or with core-like 267 GBM spheres (ratio 95:5). Scale bars 200 μm . **g** *In vitro* cell viability assay of edge-like (157, 1079, 1051, 711) and core-like (1005, 267) GBM spheres irradiated with 4Gy (IR). *** $p < 0.001$ using unpaired, two-tailed t test. Data are mean \pm s.d.; $n = 5$ independent samples per group. **h** *In vitro* cell viability assay of 101079 and 1051 edge or core GBM spheres treated with DMSO or AR42 at different concentrations. Data are mean \pm s.d.; $n = 3$ independent samples per group.



Supplementary Figure 5 HDAC1 plays a role in the protumorigenic effect of core cells and is associated with poorer clinical outcome. **a** Representative bioluminescence images of mice injected with edge-like 1051 or core-like 267 and treated with vehicle or AR42. **b** mRNA expression of C/EBP β in 59 matched longitudinal GBM samples (primary and recurrent tumors) grouped according to the expression of CD109 (up n = 30 patients or down n = 29 patients). **p<0.01 using unpaired, two-tailed t test. Data are mean \pm s.d. **c** mRNA expression of HDAC1 in the same samples as in “b” grouped according to the tumor subtype (MES n = 26, PN n = 15 and CL n = 18 independent samples). **p<0.01 using unpaired, two-tailed t test. Data are mean \pm s.d.. **d** Analysis of IHC staining intensity (H-score) for HDAC1 in recurrent GBM tissues (left) and representative image of IHC staining (right). MES n = 5 independent samples; non-MES n = 8 independent samples; The line is the median. Scale bar 200 μ m. **e** Analysis of mRNA expression of HDAC1 and HDAC2 in glioma tumor and normal brain samples from TCGA datasets, stratified according to molecular subtypes (MES n = 58, PN n = 57, Neural = 33, CL n = 54 and Normal n = 11 independent samples). ***p<0.001 using one-way ANOVA followed by Tukey’s posttest. Data are mean \pm s.d. **f** Heatmap generated from microarray data (GSE67089) showing expression of HDACs in edge-like and core-like GBM spheres, astrocytes and neural progenitor cells. **g** WB for HDAC1 using edge-like 157, 711, 1079, 1051, 374 and core-like 267, 336, 339, 1005 GBM spheres. **h** Representative immunofluorescent staining of human GBM tissues for HDAC1 (green), Olig2 (red) and DNA (blue) (upper) or for HDAC1 (green), CD109 (red) and DNA (blue) (lower). Scale bar 50 μ m.

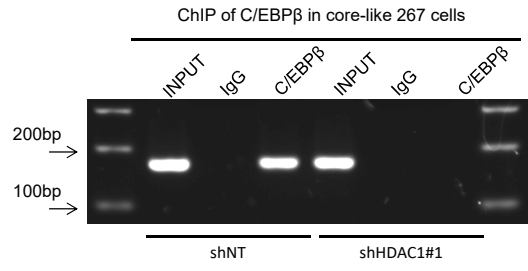
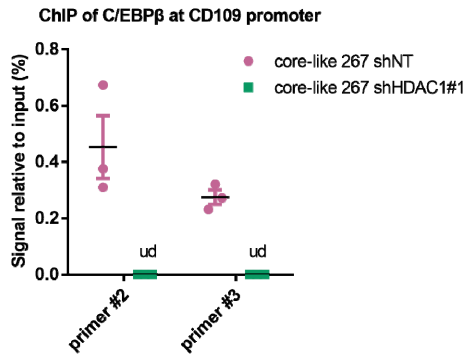


Supplementary Figure 6 Inhibition of HDAC1 attenuates the intercellular signaling from core to edge GBM cells. **a** qRT-PCR analysis for HDAC1 using core-like 267 and 1005 GBM spheres infected with lentiviruses encoding shNT or shHDAC1. *** $p < 0.001$ using one-way ANOVA followed by Dunnett's posttest. Data are mean \pm s.d.; $n = 3$ independent samples per group. **b** WB for HDAC1 using core-like 267 GBM spheres infected with lentiviruses encoding shNT or shHDAC1. **c** Fluorescence intensity of mCherry of labeled edge-like 157 GBM spheres treated with AR42 or DMSO in the presence of unlabeled edge-like 157 or core-like 267 GBM spheres. *** $p < 0.001$ using one-way ANOVA followed by Dunnett's posttest. Data are mean \pm s.d.; $n = 3$ independent samples per group. **d** GSEA of shNT infected core-like 267 or 28 GBM spheres, as compared to shHDAC1 infected spheres. Gene sets shown are DNA repair, cell cycle and spliceosome-associated genes.

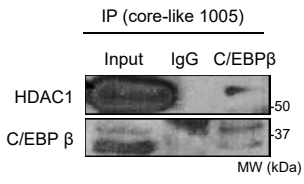


Supplementary Figure 7 Soluble CD109 is a mediator of HDAC1-derived intercellular signals from core to edge GBM cells. **a** Representative images of edge-like 157 GBM spheres treated with CM from edge-like 157 or core-like 267 GBM spheres pre-treated with proteinase K. Scale bars are 50 μ m. **b** Enzyme-linked immunosorbent assay (ELISA) of soluble CD109 in CM from edge-like 157 or core-like 20 GBM spheres. Data are mean \pm s.d.; n = 3 independent samples per group, ud – undetected. **c** ELISA of secreted CD109 in CM from core-like 267 GBM spheres with/without filtration. Data are mean \pm s.d.; n = 3 independent samples per group, ns - not significant, using unpaired, two-tailed t test. **d** Kaplan-Meier survival curve of GBM patients in IVY dataset with high or low CD109 expression in the leading edge. $p < 0.05$ using two sided log-rank test; n = 6 animals per group. **e** qRT-PCR analysis of HDAC1 expression in edge-like 157 GBM spheres infected with lentiviruses encoding GFP or HDAC1. $***p < 0.001$, using unpaired, two-tailed t test. Data are mean \pm s.d.; n = 3 independent samples per group. **f** qRT-PCR analysis of HDAC2 and CD109 expression in core-like 267 GBM spheres that were infected with shNT or shHDAC2 lentiviruses. $***p < 0.001$ using one-way ANOVA followed by Dunnett's posttest. Data are mean \pm s.d.; n = 3 independent samples per group. **g** Correlation of HDAC1 and HDAC2 with CD109 expression levels in TCGA dataset. Pearson $r = 0.444$ and $r = -0.200$ respectively. **h** *In vitro* cell viability assay of edge-like 1079 GBM spheres pretreated with recombinant CD109 and subsequently irradiated with 2Gy (IR). $*p < 0.05$, using unpaired, two-tailed t test. Data are mean \pm s.d.; n = 3 independent samples per group.

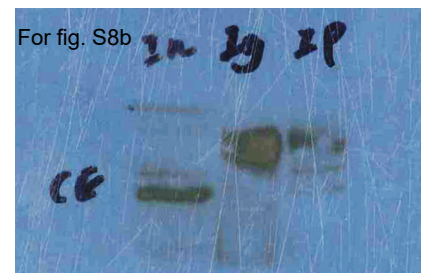
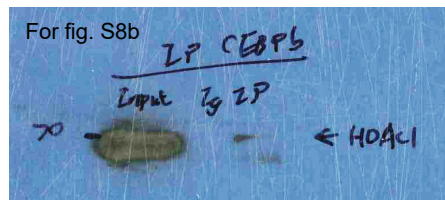
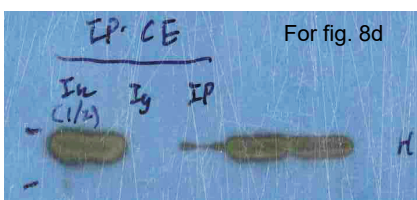
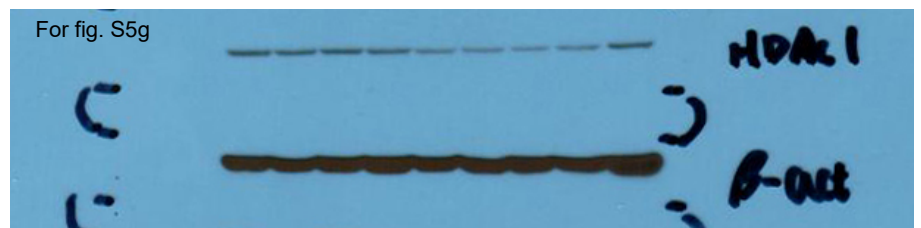
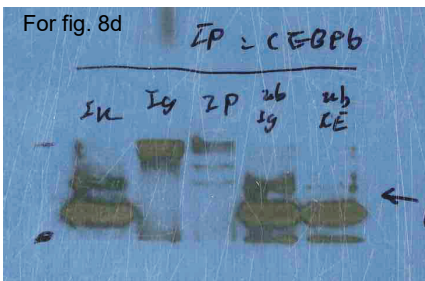
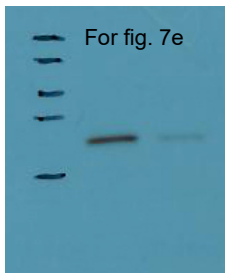
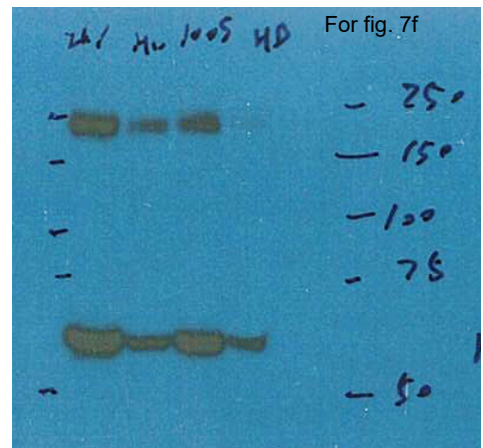
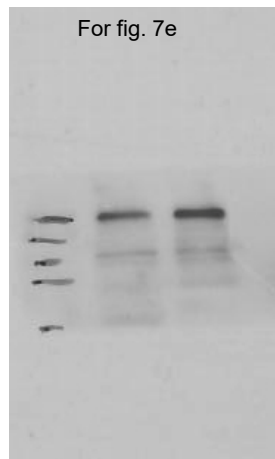
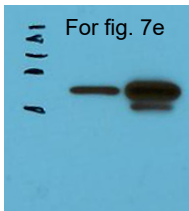
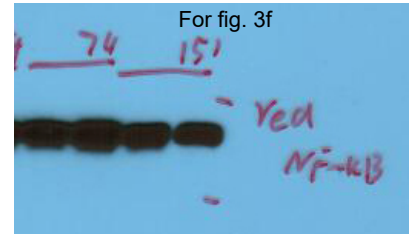
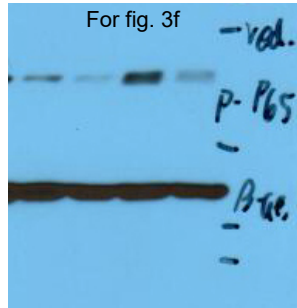
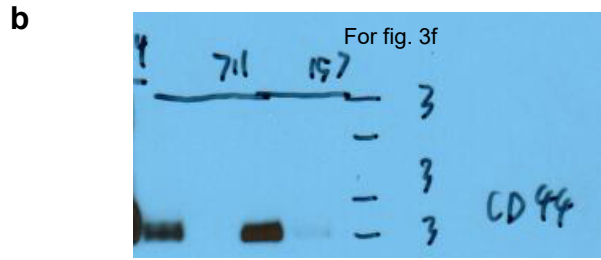
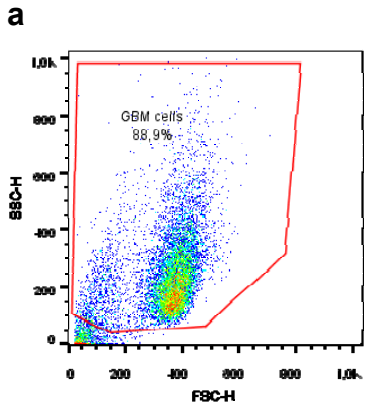
a



b



Supplementary Figure 8 HDAC1 regulates transcription of CD109 via C/EBP β . **a** ChIP analysis showing enrichment of C/EBP β at CD109 promoter region in core-like 267 GBM spheres that were infected with shNT or shHDAC1 lentiviruses (left). ud - undetected. Data are mean \pm s.d.; n = 3 independent samples per group. RT-PCR analysis of corresponding samples (right). **b** Co-immunoprecipitation of HDAC1 in core-like 1005 GBM spheres with antibodies against C/EBP β .



Supplementary Figure 9 Unprocessed data. **a** Flow cytometry gating used for apoptosis assay with CellEvent Caspase-3/7 Green Flow Cytometry Assay Kit. **b** Full scans of western blots presented in the paper.